Initial interaction of apoA-I with ABCA1 impacts in vivo metabolic fate of nascent HDL[S]

Anny Mulya,[1,*] Ji-Young Lee,[2,*] Abraham K. Gebre,[*] Elena Y. Boudyguina,[*] Soon-Kyu Chung,[*] Thomas L. Smith,[†] Perry L. Colvin,[§] Xian-Cheng Jiang,[**] and John S. Parks[3,*]

Departments of Pathology* and Orthopaedic Surgery,[†] Wake Forest University Health Sciences, Winston-Salem, NC; Division of Gerontology,[§] University of Maryland School of Medicine, and Department of Veterans Affairs and Veterans Affairs Medical Center Baltimore, Geriatric Research, Education and Clinical Center, Baltimore, MD; and Department of Anatomy and Cell Biology,** State University of New York, Downstate Medical Center, Brooklyn, NY

Abstract **We investigated the in vivo metabolic fate of pre-β HDL particles in human apolipoprotein A-I transgenic (*hA-I*^{Tg}) mice. Pre-β HDL tracers were assembled by incubation of [^{125}I]tyramine cellobiose-labeled apolipoprotein A-I (apoA-I) with HEK293 cells expressing ABCA1. Radiolabeled pre-β HDLs of increasing size (pre-β1, -2, -3, and -4 HDLs) were isolated by fast-protein liquid chromatography and injected into *hA-I*^{Tg}-recipient mice, after which plasma decay, in vivo remodeling, and tissue uptake were monitored. Pre-β2, -3, and -4 had similar plasma die-away rates, whereas pre-β1 HDL was removed 7-fold more rapidly. Radiolabel recovered in liver and kidney 24 h after tracer injection suggested increased ($P < 0.001$) liver and decreased kidney catabolism as pre-β HDL size increased. In plasma, pre-β1 and -2 were rapidly (<5 min) remodeled into larger HDLs, whereas pre-β3 and -4 were remodeled into smaller HDLs. Pre-β HDLs were similarly remodeled in vitro with control or LCAT-immunodepleted plasma, but not when incubated with phospholipid transfer protein knockout plasma.[jlr] Our results suggest that initial interaction of apoA-I with ABCA1 imparts a unique conformation that partially determines the in vivo metabolic fate of apoA-I, resulting in increased liver and decreased kidney catabolism as pre-β HDL particle size increases.—**Mulya, A., J-Y. Lee, A. K. Gebre, E. Y. Boudyguina, S-K. Chung, T. L. Smith, P. L. Colvin, X-C. Jiang, and J. S. Parks. **Initial interaction of apoA-I with ABCA1 impacts in vivo metabolic fate of nascent HDL. *J. Lipid Res.* 2008.** 49: **2390–2401.**

Supplementary key words Apolipoprotein A-I • phospholipid transfer protein • lecithin:cholesterol acyltransferase • in vivo catabolism • high density lipoproteins • ABCA1 transporter

HDLs are the smallest lipoprotein (7–12 nm in diameter) and the most dense (1.063–1.21 g/ml) of the plasma lipoprotein particles and consist of a surface monolayer of protein, phospholipid (PL), and free cholesterol surrounding a hydrophobic core of triglyceride (TG) and cholesteryl ester (CE) (1). Apolipoprotein A-I (apoA-I) is the predominant apolipoprotein on HDLs, representing 80–90% of the total protein (2). Interest in understanding HDL metabolism stems from the well-documented fact that plasma HDL cholesterol concentrations are inversely associated with coronary heart disease risk (3). This inverse association is most likely due to the role of HDLs in reverse cholesterol transport (RCT), a process in which HDLs transport excess cholesterol from peripheral tissue to the liver for secretion into bile and, ultimately, for excretion in the feces (4). However, other functions of HDL may result in protection against development of coronary heart disease, including protecting plasma LDLs from oxidation (5), decreasing inflammation (6), and improving vascular function (7).

HDLs are a heterogeneous mixture of discrete-sized particles that can be separated by density (8), size (9), electrophoretic mobility (10), and apolipoprotein content (11). Analysis of plasma HDL particles by agarose gel electrophoresis has shown that most plasma HDLs migrate in the α position (90–95% of total HDL in normal human

This work was supported by National Institutes of Health Grants HL-049373 (J.S.P.), HL-054176 (J.S.P.), and AT027820 (J.S.P.), and an American Heart Association Mid-Atlantic Affiliate Pre-doctoral Fellowship 0515420U (A.M.).

Manuscript received 9 May 2008 and in revised form 11 June 2008.

Published, JLR Papers in Press, June 25, 2008.
DOI 10.1194/jlr.M800241-JLR200

Abbreviations: ABCA1, ATP binding cassette transporter A1; apoA-I, apolipoprotein A-I; *hA-I*^{Tg}, human apolipoprotein A-I transgenic; CE, cholesteryl ester; FCR, fractional catabolic rate; FPLC, fast-protein liquid chromatography; MPM, mouse peritoneal macrophage; NDGGE, nondenaturing gradient gel electrophoresis; PL, phospholipid; PLTP, phospholipid transfer protein; RCT, reverse cholesterol transport; SR-BI, scavenger receptor class B type I; TC, tyramine cellobiose; TG, triglyceride.

[1] Present address of A. Mulya: Department of Cell Biology, Lerner Research Institute, Cleveland Clinic Foundation, Cleveland, OH 44195.

[2] Present address of J-Y. Lee: Department of Nutrition and Health Sciences, University of Nebraska, Lincoln, NE 68583.

[3] To whom correspondence should be addressed.
e-mail: jparks@wfubmc.edu

[S] The online version of this article (available at http://www.jlr.org) contains supplementary data in the form of a figure.

plasma), whereas only 5–10% migrate in the pre-β position (designated as pre-β HDL) (12). The term pre-β HDL has evolved to describe any lipoprotein that migrates in the pre-β position on agarose gel electrophoresis, including lipid-free apoA-I, lipid-poor HDL (containing only a few molecules of lipid), and discoidal HDLs (containing PL, cholesterol, and apoA-I, but no core lipid) (13, 14). Lipid-poor and discoidal HDLs are referred to as nascent HDLs because they must undergo maturation processes that ultimately result in their conversion into mature, spherical plasma HDLs containing a core of hydrophobic lipid (i.e., CE and TG). Although pre-β HDLs are minor constituents of plasma HDL, there is an intense interest in how these particles are formed and catabolized, inasmuch as several studies have suggested that pre-β HDLs are the initial acceptors of peripheral tissue cholesterol in RCT (15, 16). Despite the potential importance of pre-β HDLs in RCT, little is known about their in vivo metabolism.

We previously isolated a pre-β HDL fraction from plasma of human apoA-I transgenic (*hA-I*^{Tg}) mice using a combination of anti-human apoA-I immunoaffinity and size-exclusion chromatography and investigated its in vivo metabolism in *hA-I*^{Tg} mice (17), whose plasma HDL size heterogeneity resembles that in human plasma (18, 19). The pre-β HDL tracer isolated from *hA-I*^{Tg} mouse or human plasma, which was <7.1 nm in diameter, exhibited two metabolic fates in vivo. About 60% of the pre-β HDL tracer was rapidly removed from plasma and catabolized by the kidney, whereas the remainder was rapidly transferred to medium-sized (8.6 nm-diameter) plasma HDL particles, resulting in a slower removal rate from plasma and a preferential uptake and catabolism by the liver instead of the kidney. These results suggested that most pre-β HDLs circulating in plasma might not be nascent particles that are undergoing maturation in plasma but rather are terminal particles ready to be catabolized and incapable of mediating RCT. This concept was further supported by the absence of radiolabeled pre-β HDL in plasma after injection of small or large plasma HDL tracers into nonhuman primates or *hA-I*^{Tg} mice (17, 20).

The initial and obligatory step in HDL particle assembly is the addition of lipid to apoA-I by ABCA1, a member of the ATP binding cassette transporter family (21). The critical nature of this step for nascent HDL biogenesis and for maintaining plasma HDL cholesterol levels is demonstrated in Tangier disease subjects and ABCA1 knockout mice, both characterized by a near absence of plasma HDL (22, 23). In a recent study, we showed that incubation of apoA-I with human embryonic kidney 293 cells expressing ABCA1 (HEK293-ABCA1) is necessary and sufficient to produce at least four discrete-sized pre-β HDLs that can be isolated to apparent homogeneity (14). These pre-β HDL particles bound poorly with ABCA1 when added back to ABCA1-expressing cells, suggesting that other non-ABCA1-mediated pathways must function to add more lipids and complete the maturation process. The lack of other HDL-modifying proteins [i.e., ATP binding cassette transporter G1 (ABCG1), phospholipid transfer protein (PLTP), LCAT, apoM, or scavenger receptor class B type I (SR-BI)] in the HEK293 cells or conditioned medium of these cells suggested that the pre-β HDLs were nascent, rudimentary HDLs poised for maturation in vivo.

The purpose of the present study was to determine the in vivo plasma decay, interconversion, and tissue sites of catabolism for the ABCA1-generated nascent pre-β HDLs. Our results suggest a novel finding that the initial interaction of apoA-I with ABCA1 in vitro determines, in part, the plasma remodeling and tissue site of catabolism of these pre-β HDL particles in vivo.

METHODS

Animals

hA-I^{Tg} mice (line 427) (24) were obtained from Charles River Laboratories (Wilmington, MA). The mice were housed in the Wake Forest University Health Sciences transgenic facility and maintained on a chow diet. All protocols and procedures were approved by the Animal Care and Use Committee of Wake Forest University Health Sciences.

Isolation and iodination of apoA-I

Human HDLs were isolated by sequential ultracentrifugation of human plasma, and apoA-I was isolated from HDL by GndHCl denaturation (25, 26). The purity of the apoA-I and phosphorus content of lipid extract from 1 mg of purified apoA-I were confirmed by SDS-PAGE and the method of Fiske and Subbarow (27), respectively. ApoA-I preparations contained less than one molecule of PL per molecule of apoA-I.

ApoA-I was coupled to ^{125}I-radiolabeled tyramine cellobiose (TC) (a generous gift from Dr. Steve Adelman, Wyeth-Ayerst) as previously described (17, 28–30). Briefly, 0.01 μmol TC/mg apoA-I protein was incubated for 10 min with 5 mCi of ^{125}I (carrier-free) in a microreaction vessel coated with 20 μg Iodogen (1,3,4,6-tetrachloro-3α,6α-dephenylglycouril; Pierce Chemical Co.). The reaction was stopped by transferring the ^{125}I-radiolabeled TC to a second (iodogen-free) reaction vessel containing 10 μl of 0.1 M $NaHSO_3$ and 5 μl of 0.1 M NaI. ApoA-I was coupled to the [^{125}I]TC with cyanuric chloride (1:1 protein to TC molar ratio) by incubation at room temperature for 30 min. The [^{125}I]TC-apoA-I was then passed over a desalting column (Bio-Rad) to remove free iodine and dialyzed overnight in 0.15 M NaCl, 0.01% EDTA, pH 7.4. After removal from dialysis, the tracers were assayed for protein concentration using absorbance at 280 nm (ε = 1.13 ml/mg), and an aliquot was taken for radioactivity quantification.

Cell culture and ABCA1 expression

Human embryonic kidney (HEK)-293 ABCA1 (HEK293-ABCA1) (31) cells (gift from Dr. Michael Hayden, University of British Columbia) were maintained in DMEM supplemented with 10% FBS, 2 mM L-glutamine, 100 U/ml penicillin, 100 μg/ml streptomycin, and 50 μg/ml hygromycin B (Invitrogen). HEK293-FlpIn cells were used as negative controls and cultured in DMEM complete media in the presence of 50 μg/ml Zeocin™. Cells from a rat hepatoma cell line (McA-RH7777) were maintained in DMEM media supplemented with 10% FBS, 2 mM L-glutamine, 100 U/ml penicillin, and 100 μg/ml streptomycin.

Mouse peritoneal macrophages (MPMs) were isolated from the peritoneal cavity of C57BL/6 mice 4 days after intraperito-

neal injection of 1 ml of 10% thioglycolate. The cells obtained were washed with Media A (MEM + 10 mM HEPES) (Cellgro; Mediatech, Inc.), spun at 100 *g* for 20 min, and plated into 6-well plates at a density of 1×10^6 cells/well in MEM supplemented with 10% FBS, 100 U/ml penicillin, 100 μg/ml streptomycin, 1% MEM vitamin solution 100× (Mediatech, Inc.), and 2 mM L-glutamine. Cells were washed 2 h later and incubated overnight before use in experiments.

ABCA1 expression among the different cell types (HEK293, HEK293-ABCA1, McA-RH7777, MPM) was determined using Western blot analysis. Total cell protein was harvested using RIPA lysis buffer (50 mM Tris, 150 mM NaCl, 1% nonidet P-40, 10% sodium cholate, 1 mM EDTA) containing protease inhibitors (1 mM PMSF, 1 μg/ml pepstain, 1 μg/ml leupeptin, 1 μg/ml aprotinin). Cellular proteins (25 μg) were separated on 4–16% SDS-PAGE gels, transferred to nitrocellulose membranes (Schleicher and Schuell BioScience), and incubated for 2 h at room temperature with rabbit anti-human/mouse ABCA1 (1:1,000 dilution) (32) or anti-GAPDH monoclonal antibody (1:2,000; Santa Cruz 32233), which cross-reacts with human, rat, and mouse GAPDH. The blots were then incubated with HRP-linked anti-rabbit IgG or anti-mouse IgG (Amersham) (1:5,000 dilution) at room temperature for 1 h. Immunoblots were visualized with a chemiluminescent reagent (Pierce), and the chemiluminescence was captured with an LAS-3000 imaging system (Fujifilm Life Science) and quantified using Multi Gauge™ software.

Formation of pre-β HDL

Control (HEK293-FlpIn) and HEK293-ABCA1 cells were plated in 5 × 150 mm dishes, and McA-RH7777 cells were plated in 6-well plates and grown until they reached 95% confluence. MPMs were cultured for 2 days after isolation before experiments were initiated. All cells (HEK293, McA-RH7777, and MPMs) were washed three times with serum-free medium and then incubated with 10 μg/ml of [^{125}I]TC-apoA-I (specific activity = 5×10^4 cpm/μg) in serum-free medium for 24 h. The conditioned medium from control, ABCA1, McA-RH7777 cells, and MPMs was harvested and aliquots analyzed on 4–30% nondenaturing gradient gel electrophoresis (NDGGE). The remainder of the conditioned media was concentrated using Amicon Ultra-10 concentrators and fractionated on three Superdex 200 HR fast-protein liquid chromatography (FPLC) columns (Amersham-Biosciences) connected in series and equilibrated with 0.15 M NaCl, 0.01% EDTA, pH 7.4 (column buffer). The particles were eluted at a flow rate of 0.3 ml/min. Individual fractions were analyzed for ^{125}I radioactivity and the ^{125}I elution profile was plotted. An aliquot of each fraction of HEK293-ABCA1 cell conditioned media was analyzed by NDGGE to determine which fractions contained homogeneous-sized nascent HDL particles, after which the homogeneous-sized fractions were pooled for subsequent analyses.

In vivo turnover study

In vivo turnover studies were performed with [^{125}I]TC-pre-β HDL particles as previously described (17) with modifications. Briefly, 1.5–3 × 10^5 cpm of the radiolabeled tracer was injected into the jugular vein of anesthetized recipient *hA-I* ^{Tg} mice. Blood samples were obtained by retro-orbital bleeding at 5 min, 30 min, and 1, 2, 3, 5, and 24 h after dose injection to determine the plasma decay of radiolabeled doses. Radioactivity in a 15 μl sample of plasma was quantified using a γ counter. Aliquots of plasma from the various time points were fractionated on NDGGE for 1,100 V-h at 10°C to determine the fractional distribution of apoA-I radioactivity. After electrophoresis, gels were exposed in a phosphorimager cassette and the images were developed and quantified using a Typhoon 8600 (Molecular Dynamics, Sunnyvale, CA) and ImageQuant software (version 5.2). Twenty-four hours after tracer injection, animals were euthanized, tissues were harvested and digested with 1 N NaOH overnight at 60°C, and ^{125}I radioactivity was quantified. The remaining carcasses were digested with 10 g KOH in 150 ml of ethanol for 2–3 days; the digested carcasses were boiled in a water bath until the volume of ethanol reached about 30 ml. All remaining ethanol was counted for ^{125}I radioactivity.

Plasma volume was estimated as 3.5% of body weight, and the total amount of radiolabel in plasma at each time point was determined by multiplying the ^{125}I cpm/ml by plasma volume. For the data presented in this study, percentage of injected dose remaining in plasma at each time point was determined by dividing the amount of total radioactivity in plasma by the dose injected × 100%. Percentage of injected dose trapped in the tissue was calculated by dividing the ^{125}I radioactivity in a particular tissue by the dose injected × 100%. Fractional catabolic rate (FCR) values for HDL tracer decay from whole plasma and uptake by tissues were performed using Simulation, Analysis, and Modeling (SAAM) software, as described previously (17).

In vitro incubation study

To investigate the role of LCAT and PLTP in remodeling pre-β HDL particles, we performed an in vitro incubation study using C57BL/6 mouse plasma that had been immunodepleted of LCAT or PLTP$^{-/-}$ mouse plasma.

LCAT-immunodepleted plasma was prepared as follows. Preimmune serum and rabbit anti-mouse LCAT antisera were incubated at 56°C for 20 min to inactivate LCAT. After inactivation, either preimmune serum or rabbit anti-mouse LCAT antiserum (0.6 of plasma volume) was added to C57Bl/6 mouse plasma and incubated overnight at 4°C with rotation.

LCAT bound to IgG was pelleted by adding Protein A beads to the incubation mixture, followed by a 2 h incubation at 4°C and low-speed centrifugation. The supernatant was recovered and had 1% of the LCAT activity (33) measured in preimmune serum-treated plasma.

Twenty microliters of LCAT immunodepleted, preimmune-treated plasma, or plasma from wild-type (PLTP$^{+/+}$) or PLTP$^{-/-}$ mice was incubated with [^{125}I]TC radiolabeled pre-β1, -2, -3 and -4 HDL particles (20,000 cpm) at 4°C for 1 h or 37°C for 5 or 60 min. Subsequently, incubated plasma samples were resolved on 4–30% NDGGE and gels were analyzed by phosphorimager analysis.

In vitro reactivity of pre-β HDL with LCAT

To determine the reactivity of individual pre-β HDL particles with LCAT, pre-β1, -2, -3 and -4 HDLs were prepared using the same protocol as described above, except that cells were radiolabeled with [^{3}H]cholesterol for 24 h before incubation with apoA-I. Aliquots of pre-β1, -2, -3, and -4 HDL (10^4 dpm of [^{3}H] cholesterol) were then incubated with 50 ng of purified human recombinant LCAT in 0.5 ml of buffer (10 mM Tris, pH 7.4, 140 mM NaCl, 0.01% EDTA, 0.07% NaN_3, 0.6% BSA, 2 mM β-mercaptoethanol) at 37°C for 1 h as described previously (33, 34). After incubation, the samples were lipid-extracted and free cholesterol and CE radiolabels were separated and quantified.

Statistical analysis

Differences among the genotypes of mice were analyzed using one-way ANOVA, followed by Tukey's multiple comparison test to identify individual differences. All statistical analyses were performed using GraphPad Prism 4 (GraphPad Software, Inc., San Diego, CA).

RESULTS

Nascent pre-β HDL formation by ABCA1 cells

We previously reported that several heterogeneous-sized nascent pre-β HDL particles were generated by incubation of apoA-I with HEK293 cells stably transfected with ABCA1 (14). To evaluate whether the formation of these heterogeneous-sized nascent pre-β HDL particles was uniquely related to the level of ABCA1 overexpression in HEK293 cells, we compared ABCA1 expression and HDL particle formation using HEK293 cells stably transfected with human ABCA1, McA-RH7777 cells, and MPMs. Western blot analysis demonstrated that HEK293-ABCA1 cells expressed approximately 1.5- and 2.5-fold more ABCA1 protein compared with McA-RH7777 cells and elicited MPMs, respectively, whereas HEK293 cells had only background levels of ABCA1 expression (**Fig. 1A**). Despite the relatively modest increased level of ABCA1 protein expression in ABCA1-expressing HEK293 cells, the size distribution of nascent HDL particles was similar among the three cell types, as demonstrated by NDGGE (Fig. 1B) and high-resolution FPLC (Fig. 1C). However, the relative distribution of particles did change among cell types, with McA-RH 7777 cell medium containing a relative enrichment of larger pre-β HDL (i.e., pre-β3 and -4) (Fig. 1B). These results suggested that nascent HDLs assembled by human ABCA1 expressed in HEK293 cells were similar to those assembled by hepatoma cells and macrophages.

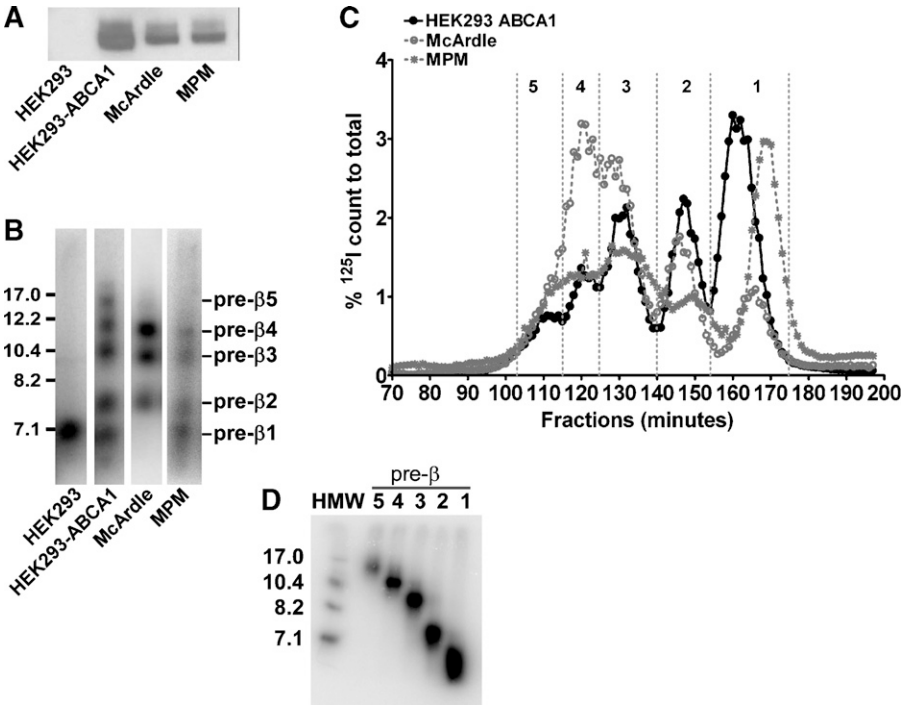

Fig. 1. Analysis of ABCA1 expression and nascent pre-β HDL size distribution from different cell types. A: ABCA1 protein expression by Western blot. Twenty-five micrograms of cell lysate protein isolated from HEK293-FlpIn cells (non-transfected control), HEK293 cells stably transfected with ABCA1, rat McArdle-RH7777 hepatoma cells, and elicited mouse peritoneal macrophages (MPMs) were separated by 4–16% SDS-PAGE. Proteins were then transferred to a nitrocellulose membrane, blotted with rabbit anti-mouse ABCA1 antisera or anti-GAPDH monoclonal antibody, and developed by chemiluminescence using an LAS-3000 imaging system (FujiFilm). Images were quantified using Multi Gauge software and normalized to GAPDH expression. For comparison among cell types, the relative expression of ABCA1 was normalized to McArdle cells. B: Nascent pre-β HDL size distribution determined by 4–30% nondenaturing gradient gel electrophoresis (NDGGE). Nontransfected (HEK293) and stably transfected (HEK293-ABCA1) cells, McArdle-RH7777 cells, and elicited MPMs were incubated with 10 μg/ml of [^{125}I]tyramine cellobiose (TC)-apolipoprotein A-I (apoA-I) for 24 h. Aliquots of conditioned media were subfractionated by NDGGE, and nascent HDLs were visualized by phosphorimager analysis. Numbers shown on left side are nm diameter. C: Nascent HDL fractionation by high-resolution fast-protein liquid chromatography (FPLC). [^{125}I]TC-apoA-I (10 μg/ml) was incubated for 24 h with the indicated cells, after which the conditioned medium was fractionated by FPLC. Radiolabel in fractions from the FPLC separation was quantified by γ counting and represented a percentage of total count recovered from the column. Vertical dashed lines denote fractions corresponding to pre-β1 to -5 HDL tracers. D: NDGGE and phosphorimager analysis of an aliquot of FPLC-fractionated pre-β1 to -5 HDL tracers generated by incubation of [^{125}I]TC-apoA-I with HEK293-ABCA1 cells for 24 h. Numbers above each lane denote pre-β HDL fraction. HMW, high-molecular-weight standard. Numbers shown on left side are nm diameter.

Preparation of nascent pre-β HDL tracer

Nascent pre-β HDL tracers for in vivo turnover studies were generated by incubating [^{125}I]tyramine cellobiose-apoA-I ([^{125}I]TC-apoA-I) with HEK293-ABCA1 cells for 24 h. ApoA-I was coupled with [^{125}I]TC, a tissue-residualizing compound, allowing us to determine tissue sites of catabolism of the injected doses. Following incubation of [^{125}I]TC-apoA-I with HEK293-ABCA-expressing cells, the conditioned medium was fractionated by FPLC, and pre-β HDL elution from the column was monitored by γ counting. As shown in Fig. 1C (black circles), five distinct peaks were eluted from post-fractionation of ABCA1 cell-conditioned medium after FPLC. Fractions for each peak were pooled, as indicated by the vertical dashed lines in Fig. 1C, and designated as pre-β1, -2, -3, -4, and -5, from the smallest to the largest particle size. Aliquots of each pool were subjected to NDGGE, and gels were developed using a phosphorimager (Fig. 1D). These results show that five discrete-sized pre-β HDLs of apparent homogeneity were isolated by the FPLC procedure. Using two-dimensional gel electrophoresis (14), we observed that all nascent HDL migrated in the pre-β position (data not shown). Sufficient amounts of pre-β1 and -4 were available for in vivo turnover studies.

Plasma turnover and tissue uptake of nascent pre-β HDLs in *hA-I^{Tg}* mice

Isolated homogeneous-sized pre-β HDLs (pre-β1, -2, -3, and -4) were injected into *hA-I^{Tg}*-recipient mice to monitor the in vivo metabolic fate of the particles. For all tracers, the injected apoA-I tracer mass was about 5 μg per animal (3×10^5 cpm per mouse/6×10^4 cpm/μg = 5 μg/mouse) and represented approximately 0.17% of the total plasma apoA-I mass in *hA-I^{Tg}* mice (plasma apoA-I pool size = ~3,000 μg) (35). Plasma was drawn from recipient mice at the indicated times to determine the kinetics of turnover of the tracers in the circulation. Plasma die-away curves for each tracer are shown in **Fig. 2A**. The plasma

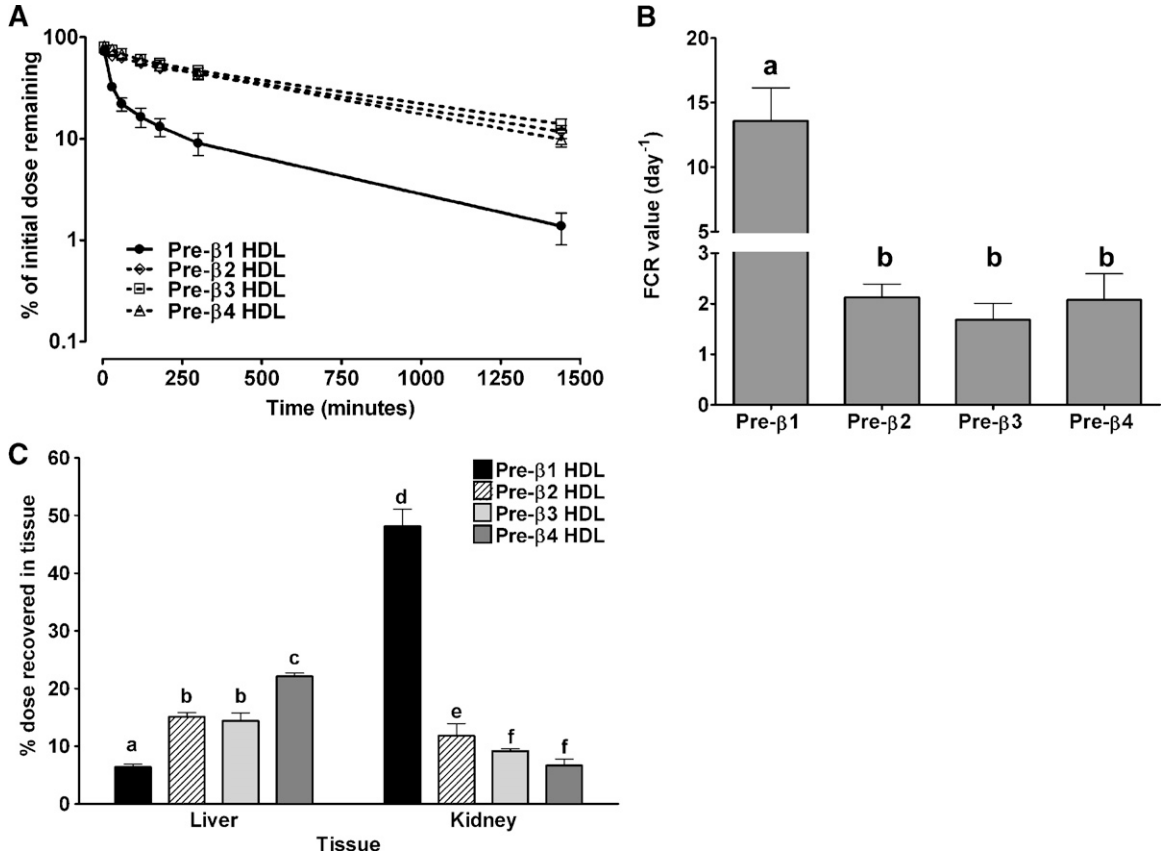

Fig. 2. Whole-plasma decay, plasma fractional catabolic rate (FCR) and tissue uptake of pre-β HDL tracers in human apolipoprotein A-I transgenic (*hA-I^{Tg}*) mice. [^{125}I]TC-pre-β1, -2, -3, and -4 HDLs were injected into *hA-I^{Tg}* mice, and plasma samples were drawn over 24 h, after which animals were euthanized and tissues were harvested and digested to quantify radiolabel uptake. Data represent mean ± SD (n = 4 for all tracers). A: Whole-plasma decay of pre-β HDL tracers in *hA-I^{Tg}* mice. Radioactivity of plasma samples at each time point was quantified and percent of injected radioactivity remaining in the plasma after dose injection was plotted versus time. B: Plasma FCR of pre-β HDL tracers in *hA-I^{Tg}* mice. FCR is expressed as pools/day. Values were calculated using SAAM software and a two-pool model with rate constants from the plasma pool to the liver and kidney, as described in the Methods section. C: Percentage of injected dose recovered in liver and kidney. Liver and kidney were harvested at the end of the study and digested overnight with 1 N NaOH at 60°C. Digested tissues were quantified for ^{125}I radioactivity and expressed as percentage of initial dose. Statistical analysis was performed using one-way ANOVA with Tukey's multiple comparison test to ascertain individual differences within a tissue. Bars with different letters are significantly different from one another at $P < 0.05$.

die-away of all tracers was similar except that of pre-β1 HDL tracer, which was cleared from the plasma significantly faster than the others. Analysis of plasma kinetic data demonstrated a 7-fold greater FCR for pre-β1 (13.58 ± 5.16 pools/day) compared with pre-β2 (2.13 ± 0.53 pools/day), pre-β3 (1.68 ± 0.66 pools/day), and pre-β4 (2.07 ± 1.04 pools/day), which were not significantly different from one another (Fig. 2B).

To identify the catabolic sites of the nascent pre-β HDL tracers in *hA-I*^{Tg} mice, tissues were removed from recipient mice 24 h after tracer injection and quantified for radiolabel uptake as percentage of injected tracer. The liver and kidney were the only organs that were quantitatively significant in the uptake and catabolism of the radiolabeled tracers and together represented >90% of radiolabel uptake (see supplementary Fig. I). Figure 2C summarizes the percentage of tissue uptake of injected tracers in the liver and kidney. In the liver, pre-β1 HDL tracer uptake was significantly less than that of pre-β2 and -3, and uptake of pre-β4 was significantly higher than the other tracers. Thus, there was a trend of increased liver tracer uptake with increasing initial nascent pre-β HDL size. The opposite trend, however, was observed for kidney uptake. Pre-β 1 tracer uptake was significantly higher than the other tracers and pre-β3 and -4 uptake was significantly lower than pre-β2. The data suggest that kidney uptake of pre-β HDL tracer was inversely related to initial pre-β HDL size.

Plasma turnover and tissue uptake of apoA-I and lipid-poor nascent pre-β1 HDLs in *hA-I*^{Tg} mice

Previously, we reported that pre-β1 HDL particles assembled by ABCA1 are similar in size, but distinct from lipid-free apoA-I in chemical composition, density, binding to ABCA1, and lipid efflux potential (14). To evaluate whether apoA-I and lipid-poor nascent pre-β1 HDLs have different in vivo metabolic fates, we compared the plasma turnover and tissue uptake of apoA-I and pre-β1 HDL tracers in *hA-I*^{Tg} mice. Pre-β1 HDL had a faster plasma turnover rate compared with apoA-I tracer, as shown in **Fig. 3A**. Analysis of plasma FCR using SAAM software showed that plasma FCR of pre-β1 HDL tracer (13.6 ± 5.2 pools/day) was 6-fold higher than that for apoA-I (2.2 ± 0.2 pools/day) (Fig. 3B), which is similar to the turnover rate of pre-β2, -3, and -4 HDL tracers (Fig. 2B). The apoA-I tracer was preferentially metabolized in the liver rather than the kidney (Fig. 3C), but the pre-β1 HDL tracer was preferentially metabolized in the kidney. These results suggest that apoA-I and lipid-poor pre-β1 HDL tracers are metabolized differently in vivo.

In vivo remodeling of nascent pre-β HDL in *hA-I*^{Tg} mice

An aliquot of plasma from each time point of the in vivo turnover study was fractionated by NDGGE, followed by phosphorimager analysis, to investigate the remodeling of each pre-β HDL subfraction during the 24 h turnover. **Figure 4** shows gel images from a representative mouse injected with [^{125}I]TC-apoA-I and pre-β1, -2, -3 and -4 HDL tracers. Unlike the plasma die-away data (Fig. 2A),

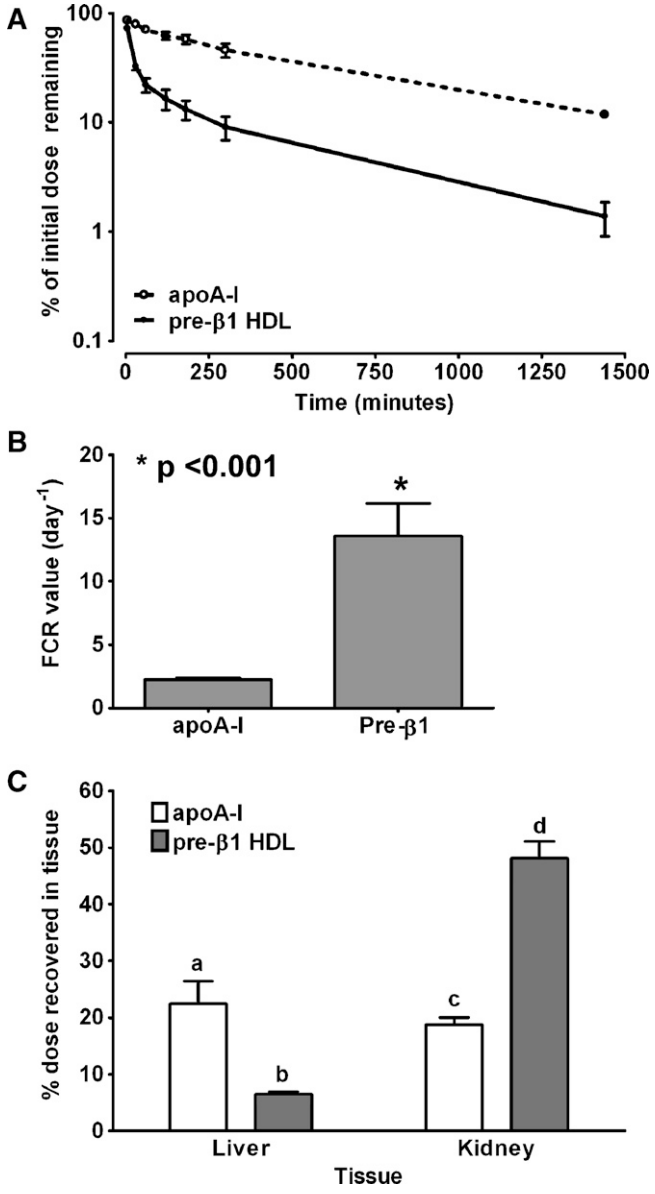

Fig. 3. Whole-plasma decay, plasma FCR, and tissue uptake of apoA-I and pre-β1 HDL tracers in *hA-I*^{Tg} mice. [^{125}I]TC-apoA-I and pre-β1 HDL tracers were injected into *hA-I*^{Tg} mice (see Fig. 2 legend). A: Whole-plasma decay of apoA-I and pre-β1 HDL tracers in *hA-I*^{Tg} mice. B: Plasma FCR of apoA-I and pre-β HDL tracers in *hA-I*^{Tg} mice. C: Percentage of injected dose recovered in liver and kidney of apoA-I and pre-β1 HDL tracers in *hA-I*^{Tg} mice. Statistical analysis was performed using one-way ANOVA with Tukey's multiple comparison test to ascertain individual differences. Bars with different letters are significantly different from one another at $P < 0.05$. Error bars indicate SEM.

HDL subfraction distribution of the remodeled pre-β HDL tracers in plasma was more complicated. At the earliest time point examined (5 min), nearly all of the radiolabeled apoA-I was distributed in the medium HDL size range (8–10 nm in diameter), and this distribution varied little over the 24 h time course of the study (Fig. 4, upper left panel). In contrast, at the 5 min time point, some of the pre-β1 HDL tracer was distributed in the medium HDL size range, whereas some remained in the pre-β1 size range (<7.1 nm)

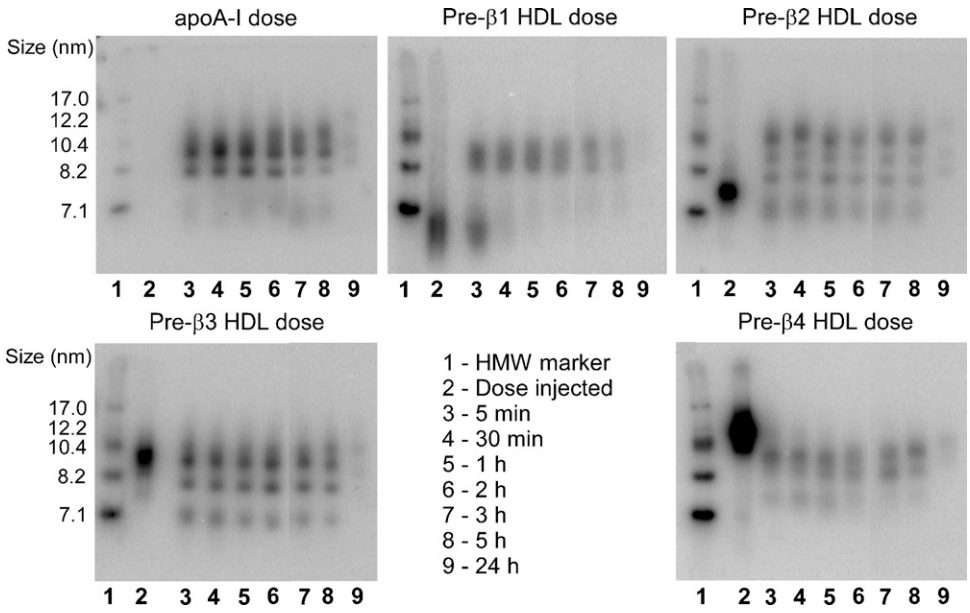

Fig. 4. Size distribution of pre-β HDL tracers after intravenous injection into *hA-I*^{Tg}-recipient mice. Plasma samples were harvested at the indicated times after [^{125}I]TC-apoA-I and pre-β1, -2, -3, and -4 HDL tracer injection. Plasma samples (15 μl aliquot) were fractionated on 4–30% NDGGE, and radiolabel distribution was visualized using a phosphorimager. A phosphorimager result of one representative recipient mouse for each tracer is shown. HMW protein standard (lane 1) and dose (lane 2) are shown for reference. Lanes 3–9 contain plasma samples taken at 5 min, 30 min, and 1, 2, 3, 5, and 24 h, respectively.

(Fig. 4, upper middle panel). This pattern of in vivo remodeling resembled that in a previous study using plasma-isolated pre-β HDL (17). The pre-β2 HDL tracer remodeled into at least four distinct HDL size ranges between 7 and 13 nm in diameter, three of which were larger than the injected tracer (Fig. 4, upper right panel). In contrast, the pre-β3 HDL tracer was distributed into three distinct size ranges between 7 and 10.4 nm in diameter, one of which was similar in size to the injected pre-β3 HDL (Fig. 4, lower left panel). Pre-β4 HDL tracer was distributed into three smaller HDL particles, <10 nm in diameter, all of which were smaller than the original pre-β4 HDL tracer (Fig. 4, lower right panel). Thus, even though the whole-plasma decay for pre-β2, -3, and -4 HDL tracers was similar, the remodeling of these tracers in plasma was distinctly different, with apoA-I and pre-β1 and -2 remodeled into larger particles and pre-β3 and -4 remodeled into smaller particles.

Using phosphorimager analysis of NDGGE data similar to those in Fig. 4, we quantified the amount of radiolabel associated with particles <7.1 nm in diameter and particles in the medium HDL size range (8–10 nm) for each time point of the apoA-I and pre-β1 HDL tracer turnover studies (using ImageQuant Software), followed by analysis with the SAAM II program. Five minutes after injection, 62.6% of the pre-β1 tracer remained as pre-β1 (<7.1 nm), and was removed from the circulation at an extraordinarily rapid rate (FCR 92.92 ± 5.85 pools/day); the remaining 22.8% of pre-β1 tracer was remodeled to medium-sized HDLs, which were removed from circulation much more slowly (FCR 7.76 ± 4.75 pools/day). Additional analyses suggested that as much as 97.7% of radioactivity found in kidney of animals injected with pre-β1 HDL tracers could be accounted for by the pre-β1 tracer, which was rapidly removed from circulation and not converted to larger particles during the first 5 min after injection (data not shown). This suggests that pre-β1 HDL particles not immediately converted to or associated with medium-sized HDL within 5 min after injection are removed rapidly from circulation by the kidney. Kinetic analysis also suggested that radioactivity recovered in the liver of mice injected with pre-β1 HDL tracer was derived almost exclusively from pre-β1 tracer that was remodeled into medium-sized HDL. Similar kinetic results were observed for plasma-isolated pre-β HDL in our previous study (17).

In vitro remodeling of nascent pre-β HDL tracers

To determine whether HDL-remodeling factors such as LCAT (36) and PLTP (37, 38) promote nascent pre-β HDL remodeling in vivo, we performed in vitro incubations of mouse plasma with nascent pre-β HDL tracers. To investigate the role of LCAT, we performed an in vitro incubation of nascent pre-β HDL tracers with either control or LCAT-immunodepleted plasma. LCAT was immunodepleted from plasma using anti-mouse LCAT antibody, which reduced LCAT activity by 99% compared with preimmune serum-incubated plasma (control). The role of PLTP in nascent pre-β HDL remodeling was also investigated by incubation of nascent pre-β HDL tracers in wild-type versus PLTP$^{-/-}$ mouse plasma. Because most of the in vivo remodeling occurred within the first hour after tracer injection, each tracer was incubated with plasma for 5 or 60 min at 37°C, or 60 min at 4°C as a control. At the

end of incubation, plasma samples were fractionated by NDGGE and phosphorimager analysis was performed to follow the tracer remodeling. A representative experiment is shown in **Fig. 5**. No apparent remodeling of any pre-β HDL tracer occurred with 60 min incubation at 4°C (lanes 2 and 3 for each gel in top and bottom panel). However, incubation of pre-β HDLs in control plasma for 5 min (lane 4) or 60 min (lane 6) at 37°C resulted in remodeling to medium-sized HDL (8–10 nm) for pre-β1 and -2 tracer and remodeling to small HDL (7–8 nm) for pre-β3 and -4 tracers. In the absence of active LCAT (Fig. 5, top panel), tracer remodeling was still observed with 5 min (lanes 4 vs. 5) and 60 min (lane 6 vs. 7) incubations at 37°C, suggesting that LCAT is not an absolute requirement for remodeling of nascent pre-β HDL. A different result was observed in the absence of PLTP. Remodeling of all nascent pre-β HDL tracers at 37°C was significantly decreased in PLTP$^{-/-}$ plasma (Fig. 5, lower panel, lanes 5 and 7) compared with wild-type control plasma (Fig. 5, lower panel, lanes 4 and 6), suggesting that PLTP is necessary for remodeling of nascent pre-β HDL.

In vitro reactivity of pre-β HDL with LCAT

To determine LCAT reactivity with each pre-β HDL particle, we performed in vitro incubations using purified human recombinant LCAT (**Fig. 6**). All pre-β HDL particles were reactive with LCAT, and particle reactivity increased with increasing pre-β HDL size.

DISCUSSION

Pre-β HDLs represent 5–10% of the plasma HDL pool (12) and are the nascent precursor particles to mature, spherical HDLs. The formation of pre-β HDL particles by ABCA1 is the first committed step in HDL formation and results in particles that can participate in RCT by removing excess cholesterol from tissues. Despite the importance of pre-β HDLs as intermediates in HDL particle formation and RCT, very little is known about their metabolism in vivo. We showed previously that addition of apoA-I to cells expressing ABCA1 results in the formation of up to five distinct pre-β HDL subfractions with increasing size and lipid-to-protein ratios (14). The goal of this study was to determine the in vivo metabolic fate of these pre-β HDLs. Surprisingly, the removal rate of pre-β HDLs from plasma was very similar for pre-β2, -3, and -4 HDL tracers and comparable with apoA-I tracer, but was much faster for pre-β1 HDL. Although the plasma die-away curves were similar among the larger pre-β HDLs (i.e., -2, -3, and -4), intravascular remodeling of the pre-β HDL tracer after injection was complex, with pre-β1 and -2 remodeled predominantly into larger particles and pre-β3

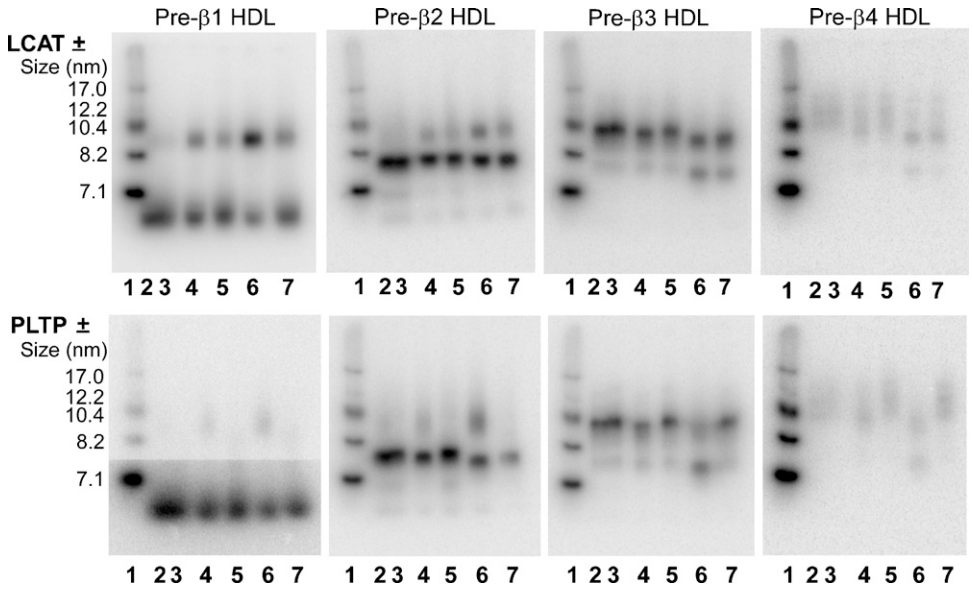

Fig. 5. In vitro remodeling of pre-β HDL tracers in the presence or absence of LCAT or PLTP. [^{125}I]TC-radiolabeled pre-β1 to -4 HDLs were incubated with plasma with or without LCAT (top panel) or PLTP (lower panel). C57Bl/6 mouse plasma was incubated with anti-mouse LCAT antiserum to immunodeplete LCAT or preimmune serum (control) (see Methods section). LCAT immunodepletion was >99% compared with preimmune incubated plasma. Plasma from wild-type (WT) or PLTP$^{-/-}$ plasma was used to investigate pre-β HDL remodeling in the presence or absence of PLTP. Incubations were performed for 1 h at 4°C or for 5 min and 1 h at 37°C. Aliquots of the incubation mixtures were subjected to 4–30% NDGGE and developed with a phosphorimager. Top panel, incubations ± LCAT; bottom panel, incubations ± PLTP. 1: HMW marker; hydrodynamic size of standard proteins is shown on the left; 2: WT, 4°C, 1 h; 3: LCAT-depleted (−LCAT) or PLTP$^{-/-}$, 4°C, 1 h; 4: WT, 37°C, 5 min; 5: −LCAT or PLTP$^{-/-}$, 37°C, 5 min; 6: WT, 37°C, 1 h; 7: −LCAT or PLTP$^{-/-}$, 37°C, 1 h.

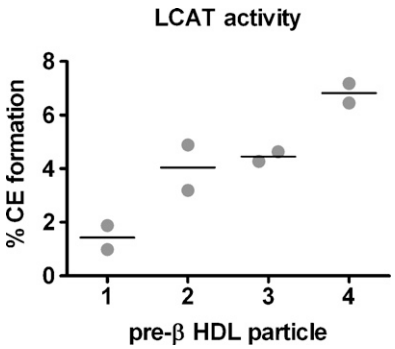

Fig. 6. In vitro reactivity of pre-β HDL with human LCAT. Individual pre-β HDLs were assembled and isolated (see Fig. 1 legend). An equal amount of pre-β HDL cholesterol (10^4 dpm) was incubated with 50 ng of purified human recombinant LCAT at 37°C for 1 h (see Methods). The incubation mixtures were then lipid extracted and the percentage of radiolabeled free cholesterol converted to cholesteryl ester was determined. The percentage cholesterol esterification in the absence of added LCAT enzyme (i.e., blank) was measured and subtracted from that measured in the presence of LCAT for each pre-β HDL particle. Results present duplicate incubations, with the horizontal line denoting the average value of the duplicates.

and -4 remodeled into smaller particles. The nature of this rapid remodeling is unknown; however, it appears to be dependent on PLTP activity, but not LCAT activity, even though we show that the pre-β HDLs are reactive with LCAT in vitro (Fig. 6). Finally, despite the differences in remodeling, the tissue uptake of pre-β HDLs was related to the initial particle size assembled by ABCA1, such that as initial pre-β HDL size increased, more particles were taken up by the liver and fewer by the kidney. Given these results, larger pre-β HDLs would seem likely to accept more cholesterol from peripheral tissue and to be preferentially taken up by the liver. Even though selective cholesterol uptake (i.e., uptake of core CE without whole-particle uptake) makes a greater contribution to RCT than whole-particle HDL uptake by the liver (39), increased uptake and degradation of HDL particles would still enhance RCT. Thus, our studies suggest that the initial interaction of apoA-I with ABCA1 is necessary to assemble pre-β HDLs and also appears to predetermine, to some extent, the ultimate in vivo metabolic fate of pre-β HDLs.

Studies in Tangier subjects and ABCA1 gene-targeted mice have shown that ABCA1 is absolutely required for HDL formation (22, 23). It is now clear that ABCA1 functions to assemble apoA-I with cellular lipid to form nascent pre-β HDLs (40, 41). We and others have shown that incubation of apoA-I with cells expressing ABCA1 is necessary and sufficient to generate multiple-sized pre-β HDL subfractions that appear to be formed simultaneously in cell culture media (14, 42–45). We observed that these pre-β HDLs, once formed and isolated, are poor substrates for subsequent binding to ABCA1 and lipid efflux (14, 46), suggesting that the initial interaction of ABCA1 with apoA-I or the addition of lipid to apoA-I via ABCA1 results in a conformational constraint in apoA-I that diminishes its ability for subsequent interaction with ABCA1. A corollary to this observation is that addition of lipid to these pre-β HDLs requires other proteins, such as PLTP, ABCG1, and/or SR-BI, to undergo further maturation; this idea has been supported by direct experimentation (47–49). Our current study extends these findings to in vivo metabolism and suggests that the initial interaction of apoA-I with ABCA1 results in a type of "metabolic imprinting" that predetermines the tissue site of uptake of the pre-β HDLs. For instance, we found similar plasma die-away curves for pre-β2 and -4 HDLs (Fig. 2A, B). However, in plasma, pre-β2 HDL is remodeled into larger particles, on average, whereas pre-β4 HDL is remodeled into smaller ones. Despite this intravascular remodeling, which results in some overlapping particle size ranges for pre-β2 and pre-β4 HDL tracers (Fig. 4), significantly more of the pre-β4 tracer is removed from circulation by the liver and less by the kidney, compared with pre-β2 (Fig. 2). In other words, the larger the pre-β HDL produced by the interaction of apoA-I with ABCA1, the more likely is the nascent pre-β HDL to be catabolized by the liver, in what probably is one of the final steps in HDL particle RCT. Thus, our study suggests a role for ABCA1 in determining the metabolic fate of pre-β HDL in vivo, which may influence the degree to which pre-β HDLs participate in whole-particle RCT.

Pre-β1 HDLs, sometimes referred to as lipid-poor apoA-I, are distinct from other pre-β HDLs and from lipid-free apoA-I. Our previous studies have documented that pre-β 1 HDLs contain only a few molecules of PL and one molecule of apoA-I (14, 17). We observed that despite the very low lipid content, isolated pre-β1 HDLs bind poorly to ABCA1 and are poor acceptors for lipid efflux, suggesting that apoA-I conformation has been constrained by its initial interaction with ABCA1 (14). Indeed, thermal denaturation of pre-β1 by heating to 60°C for 30 min resulted in partial recovery of binding, supporting the concept that the constrained conformation of apoA-I induced by interaction with ABCA1 is relieved by thermal unfolding, which allows recovery of binding to ABCA1 (14). Recently, Duong et al. (50) reported the formation of a similar lipid-poor pre-β1 HDL population by skin fibroblasts in which ABCA1 activity was stimulated by 9-*cis*-retinoic acid and 22-hydroxycholesterol. However, in their study, pre-β1 HDL particles effluxed cholesterol as efficiently as lipid-free apoA-I. The apparent discrepancy in results may be related to small differences in PL content due to differences in incubation time, or other experimental variables (i.e., cell type, level of ABCA1 expression). The combined results suggest a critical amount of PL may be necessary to "constrain" apoA-I on pre-β1 HDL into a conformation that no longer allows interaction with ABCA1 and lipid efflux.

The in vivo metabolism of pre-β1 HDLs is also distinct from that of other pre-β HDL particles and lipid-free apoA-I. Pre-β1 HDLs are rapidly removed from plasma by the kidney and are not likely to undergo extensive remodeling in plasma. The remodeling of some of the pre-β1 tracer to medium-sized HDL may stem from the presence of lipid-free apoA-I in the preparation, which

cannot be distinguished or separated from pre-β1 HDL by existing experimental methodologies. In fact, the most sensitive measurement of lipid-free apoA-I content in the pre-β1 HDL preparation appears to be the rapid remodeling of radiolabel to medium-sized HDLs, because we have shown here (Fig. 4) and previously (17) that radiolabeled lipid-free apoA-I is transferred quantitatively to medium-sized HDLs within 5 min after injection into recipient mice. Unlike lipid-free apoA-I, which can readily and rapidly transfer to medium-sized HDLs (17, 51), pre-β1 HDLs appear unable to do so. We speculate that a few molecules of PL in pre-β1 HDL are enough to stabilize the structure of apoA-I, preventing its interaction with ABCA1 and its association or transfer to preexisting plasma HDL particles. Taken together, our results suggest that pre-β1 HDLs in plasma are terminal particles that are not sufficiently lipidated by ABCA1 to prevent their premature removal from the circulation by the kidney. Insufficient lipidation of apoA-I may occur due to limited availability of ABCA1 expression on the cell surface, limited availability of cellular lipid, or both. If our hypothesis is correct, any perturbation that results in additional lipidation of apoA-I to produce relatively more pre-β2, -3, or -4 HDLs, rather than pre-β1, will result in a proportional increase in catabolism of pre-β HDLs by the liver and may enhance HDL whole-particle RCT.

Another novel and surprising finding of our study was the remodeling of pre-β HDL tracers in plasma after injection. Subsequent studies showed that tracer remodeling also occurred with in vitro incubation in plasma, demonstrating that the remodeling factors were available in plasma. Although the molecular nature of this remodeling process is unknown, it requires active PLTP (Fig. 5), which has been shown to remodel plasma HDL particles into larger and smaller HDL products (37, 38). Interestingly, we observed in our in vivo and in vitro studies that pre-β1 and -2 HDLs were remodeled into larger particles, whereas pre-β3 and -4 HDLs were remodeled into smaller, average-sized HDLs. The very rapid nature of the remodeling (<5 min) suggested that it might involve pre-β HDL fusion with, or transfer to, preexisting plasma HDL particles. However, the data do not support random exchange of radiolabeled apoA-I, inasmuch as remodeling occurred in discrete size ranges of HDL (Figs. 4, 5), not throughout the entire range of particle sizes, and required PLTP and 37°C incubation. We also observed that pre-β HDL particles were reactive with LCAT (Fig. 6); however, LCAT activity was not necessary for remodeling. A similar conclusion was reached in our previous study, in which in vitro remodeling of plasma isolated pre-β HDLs, which were similar in size and composition to the pre-β1 HDLs in this study, occurred unabated in the presence of an LCAT inhibitor (35). These data do not contradict the essential role for LCAT in the maturation of nascent discoidal pre-β HDLs to spherical plasma HDLs through cholesterol esterification (52–55). Rather, they suggest that cholesterol esterification was not a necessary prerequisite for rapid remodeling in our study. Other plasma factors that have been shown to remodel HDL particles, such as CE transfer protein and hepatic lipase, were not investigated in the present study (13). Further studies are required to define the molecular nature of the rapid remodeling of ABCA1-generated pre-β HDLs in plasma.

To our knowledge, this is the first study to define the in vivo metabolic fate of pre-β HDL particles assembled by ABCA1, and the results fill some critical gaps in our knowledge regarding HDL metabolism. It is now clear from our studies in tissue-specific ABCA1 knockout mice that nearly all of the plasma HDL pool can be accounted for by liver and intestinal production (32, 57). It is also interesting that only these two tissues quantitatively produce apoA-I (56). There is also mounting evidence that assembly of most HDL particles occurs at the cell surface (45, 58–64) or in a recycling endosomal compartment by ABCA1 (65–70) and not in the secretory pathway of the endoplasmic reticulum and Golgi apparatus (71). Because we have shown that poorly lipidated apoA-I (i.e., pre-β1 HDL) is rapidly catabolized by the kidney, whereas lipid-free apoA-I rapidly and quantitatively transfers to plasma HDLs (17, 51), newly synthesized apoA-I from hepatocytes or intestinal epithelial cells has several metabolic fates. If apoA-I escapes lipidation in the secretory pathway and at the cell surface by ABCA1, it is likely to associate with mature HDL particles after entering the circulation (17, 51). If lipidation in the secretory pathway or at the cell surface by ABCA1 is sufficient to form pre-β2, -3, or -4 HDLs, these particles will undergo further lipidation by non-ABCA1-mediated pathways and ultimately be converted to mature plasma HDL particles by LCAT in plasma. If, on the other hand, apoA-I is poorly lipidated, with only a few molecules of PL in the secretory pathway or by ABCA1 at the cell surface, it will not contain enough lipid to prevent its rapid clearance from plasma by the kidney. Thus, increasing hepatic or intestinal ABCA1 expression in the absence of increased lipid availability or increasing hepatic or intestinal apoA-I secretion in the absence of increased ABCA1 expression may not result in a proportional increase in plasma HDL concentration.

The authors thank Dr. Michael Hayden from the University of British Columbia, Vancouver, Canada for providing us with ABCA1-expressing cells.

REFERENCES

1. Atkinson, D., and D. M. Small. 1986. Recombinant lipoproteins: implications for structure and assembly of native lipoproteins. *Annu. Rev. Biophys. Biophys. Chem.* **15:** 403–456.
2. Eisenberg, S. 1984. High density lipoprotein metabolism. *J. Lipid Res.* **25:** 1017–1058.
3. Gordon, D. J., J. L. Probstfield, R. J. Garrison, J. D. Neaton, W. P. Castelli, J. D. Knoke, D. R. Jacobs, Jr., S. Bangdiwala, and H. A. Tyroler. 1989. High-density lipoprotein cholesterol and cardiovascular disease. Four prospective American studies. *Circulation.* **79:** 8–15.
4. Fielding, C. J., and P. E. Fielding. 1995. Molecular physiology of reverse cholesterol transport. *J. Lipid Res.* **36:** 211–228.
5. Nofer, J. R., B. Kehrel, M. Fobker, B. Levkau, G. Assmann, and A. von Eckardstein. 2002. HDL and arteriosclerosis: beyond reverse cholesterol transport. *Atherosclerosis.* **161:** 1–16.

6. Xia, P., M. A. Vadas, K. A. Rye, P. J. Barter, and J. R. Gamble. 1999. High density lipoproteins (HDL) interrupt the sphingosine kinase signaling pathway. A possible mechanism for protection against atherosclerosis by HDL. *J. Biol. Chem.* **274:** 33143–33147.
7. Yuhanna, I. S., Y. Zhu, B. E. Cox, L. D. Hahner, S. Osborne-Lawrence, P. Lu, Y. L. Marcel, R. G. Anderson, M. E. Mendelsohn, H. H. Hobbs, et al. 2001. High-density lipoprotein binding to scavenger receptor-BI activates endothelial nitric oxide synthase. *Nat. Med.* **7:** 853–857.
8. Anderson, D. W., A. V. Nichols, T. M. Forte, and F. T. Lindgren. 1977. Particle distribution of human serum high density lipoproteins. *Biochim. Biophys. Acta.* **493:** 55–68.
9. Blanche, P. J., E. L. Gong, T. M. Forte, and A. V. Nichols. 1981. Characterization of human high-density lipoproteins by gradient gel electrophoresis. *Biochim. Biophys. Acta.* **665:** 408–419.
10. Kunitake, S. T., K. J. La Sala, and J. P. Kane. 1985. Apolipoprotein A-I-containing lipoproteins with pre-beta electrophoretic mobility. *J. Lipid Res.* **26:** 549–555.
11. Cheung, M. C., and J. J. Albers. 1984. Characterization of lipoprotein particles isolated by immunoaffinity chromatography. Particles containing A-I and A-II and particles containing A-I but no A-II. *J. Biol. Chem.* **259:** 12201–12209.
12. O'Connor, P. M., B. R. Zysow, S. A. Schoenhaus, B. Y. Ishida, S. T. Kunitake, J. M. Naya-Vigne, P. N. Duchateau, R. F. Redberg, S. J. Spencer, S. Mark, et al. 1998. Prebeta-1 HDL in plasma of normolipidemic individuals: influences of plasma lipoproteins, age, and gender. *J. Lipid Res.* **39:** 670–678.
13. Rye, K. A., and P. J. Barter. 2004. Formation and metabolism of prebeta-migrating, lipid-poor apolipoprotein A-I. *Arterioscler. Thromb. Vasc. Biol.* **24:** 421–428.
14. Mulya, A., J. Y. Lee, A. K. Gebre, M. J. Thomas, P. L. Colvin, and J. S. Parks. 2007. Minimal lipidation of pre-beta HDL by ABCA1 results in reduced ability to interact with ABCA1. *Arterioscler. Thromb. Vasc. Biol.* **27:** 1828–1836.
15. Castro, G. R., and C. J. Fielding. 1988. Early incorporation of cell-derived cholesterol into pre-beta-migrating high-density lipoprotein. *Biochemistry.* **27:** 25–29.
16. Huang, Y., A. von Eckardstein, and G. Assmann. 1993. Cell-derived unesterified cholesterol cycles between different HDLs and LDL for its effective esterification in plasma. *Arterioscler. Thromb.* **13:** 445–458.
17. Lee, J. Y., L. Lanningham-Foster, E. Y. Boudyguina, T. L. Smith, E. R. Young, P. L. Colvin, M. J. Thomas, and J. S. Parks. 2004. Prebeta high density lipoprotein has two metabolic fates in human apolipoprotein A-I transgenic mice. *J. Lipid Res.* **45:** 716–728.
18. Chajek-Shaul, T., T. Hayek, A. Walsh, and J. L. Breslow. 1991. Expression of the human apolipoprotein A-I gene in transgenic mice alters high density lipoprotein (HDL) particle size distribution and diminishes selective uptake of HDL cholesteryl esters. *Proc. Natl. Acad. Sci. USA.* **88:** 6731–6735.
19. Rubin, E. M., B. Y. Ishida, S. M. Clift, and R. M. Krauss. 1991. Expression of human apolipoprotein A-I in transgenic mice results in reduced plasma levels of murine apolipoprotein A-I and the appearance of two new high density lipoprotein size subclasses. *Proc. Natl. Acad. Sci. USA.* **88:** 434–438.
20. Colvin, P. L., E. Moriguchi, P. H. R. Barrett, J. S. Parks, and L. L. Rudel. 1999. Small HDL particles containing two apoA-I molecules are precursors in vivo to medium and large HDL particles containing three and four apoA-I molecules in nonhuman primates. *J. Lipid Res.* **40:** 1782–1792.
21. Yokoyama, S. 2000. Release of cellular cholesterol: molecular mechanism for cholesterol homeostasis in cells and in the body. *Biochim. Biophys. Acta.* **1529:** 231–244.
22. Fredrickson, D. S. 1964. The inheritance of high density lipoprotein deficiency (Tangier disease). *J. Clin. Invest.* **43:** 228–236.
23. McNeish, J., R. J. Aiello, D. Guyot, T. Turi, C. Gabel, C. Aldinger, K. L. Hoppe, M. L. Roach, L. J. Royer, J. de Wet, et al. 2000. High density lipoprotein deficiency and foam cell accumulation in mice with targeted disruption of ATP-binding cassette transporter-1. *Proc. Natl. Acad. Sci. USA.* **97:** 4245–4250.
24. Walsh, A., Y. Ito, and J. L. Breslow. 1989. High levels of human apolipoprotein A-I in transgenic mice result in increased plasma levels of small high density lipoprotein (HDL) particles comparable to human HDL3. *J. Biol. Chem.* **264:** 6488–6494.
25. Nichols, A. V., E. L. Gong, P. J. Blanche, T. M. Forte, and D. W. Anderson. 1976. Effects of guanidine hydrochloride on human plasma high density lipoproteins. *Biochim. Biophys. Acta.* **446:** 226–239.
26. Parks, J. S., and L. L. Rudel. 1979. Isolation and characterization of high density lipoprotein apoproteins in the non-human primate (vervet). *J. Biol. Chem.* **254:** 6716–6723.
27. Fiske, C. H., and Y. Subbarow. 1925. Colorimetric determination of phosphorus. *J. Biol. Chem.* **66:** 375–400.
28. Pittman, R. C., T. E. Carew, C. K. Glass, S. R. Green, C. A. Taylor, Jr., and A. D. Attie. 1983. A radioiodinated, intracellularly trapped ligand for determining the sites of plasma protein degradation in vivo. *Biochem. J.* **212:** 791–800.
29. Glass, C. K., R. C. Pittman, G. A. Keller, and D. Steinberg. 1983. Tissue sites of degradation of apoprotein A-I in the rat. *J. Biol. Chem.* **258:** 7161–7167.
30. Huggins, K. W., E. R. Burleson, J. K. Sawyer, K. Kelly, L. L. Rudel, and J. S. Parks. 2000. Determination of the tissue sites responsible for the catabolism of large high density lipoprotein in the African green monkey. *J. Lipid Res.* **41:** 384–394.
31. See, R. H., R. A. Caday-Malcolm, R. R. Singaraja, S. Zhou, A. Silverston, M. T. Huber, J. Moran, E. R. James, R. Janoo, J. M. Savill, et al. 2002. Protein kinase A site-specific phosphorylation regulates ATP-binding cassette A1 (ABCA1)-mediated phospholipid efflux. *J. Biol. Chem.* **277:** 41835–41842.
32. Timmins, J. M., J. Y. Lee, E. Boudyguina, K. D. Kluckman, L. R. Brunham, A. Mulya, A. K. Gebre, J. M. Coutinho, P. L. Colvin, T. L. Smith, et al. 2005. Targeted inactivation of hepatic Abca1 causes profound hypoalphalipoproteinemia and kidney hypercatabolism of apoA-I. *J. Clin. Invest.* **115:** 1333–1342.
33. Parks, J. S., A. K. Gebre, and J. W. Furbee. 1999. Lecithin-cholesterol acyltransferase. Assay of cholesterol esterification and phospholipase A2 activities. *Methods Mol. Biol.* **109:** 123–131.
34. Chisholm, J. W., A. K. Gebre, and J. S. Parks. 1999. Characterization of C-terminal histidine-tagged human recombinant lecithin: cholesterol acyltransferase. *J. Lipid Res.* **40:** 1512–1519.
35. Lee, J. Y., J. M. Timmins, A. Mulya, T. L. Smith, Y. Zhu, E. M. Rubin, J. W. Chisholm, P. L. Colvin, and J. S. Parks. 2005. HDLs in apoA-I transgenic Abca1 knockout mice are remodeled normally in plasma but are hypercatabolized by the kidney. *J. Lipid Res.* **46:** 2233–2245.
36. Nakamura, Y., L. Kotite, Y. Gan, T. A. Spencer, C. J. Fielding, and P. E. Fielding. 2004. Molecular mechanism of reverse cholesterol transport: reaction of pre-beta-migrating high-density lipoprotein with plasma lecithin/cholesterol acyltransferase. *Biochemistry.* **43:** 14811–14820.
37. Jauhiainen, M., J. Metso, R. Pahlman, S. Blomqvist, A. van Tol, and C. Ehnholm. 1993. Human plasma phospholipid transfer protein causes high density lipoprotein conversion. *J. Biol. Chem.* **268:** 4032–4036.
38. Settasatian, N., M. Duong, L. K. Curtiss, C. Ehnholm, M. Jauhiainen, J. Huuskonen, and K. A. Rye. 2001. The mechanism of the remodeling of high density lipoproteins by phospholipid transfer protein. *J. Biol. Chem.* **276:** 26898–26905.
39. Trigatti, B., A. Rigotti, and M. Krieger. 2000. The role of the high-density lipoprotein receptor SR-BI in cholesterol metabolism. *Curr. Opin. Lipidol.* **11:** 123–131.
40. Francis, G. A., R. H. Knopp, and J. F. Oram. 1995. Defective removal of cellular cholesterol and phospholipids by apolipoprotein A-I in Tangier Disease. *J. Clin. Invest.* **96:** 78–87.
41. Remaley, A. T., U. K. Schumacher, J. A. Stonik, B. D. Farsi, H. Nazih, and H. B. Brewer, Jr. 1997. Decreased reverse cholesterol transport from Tangier disease fibroblasts. Acceptor specificity and effect of brefeldin on lipid efflux. *Arterioscler. Thromb. Vasc. Biol.* **17:** 1813–1821.
42. Duong, P. T., H. L. Collins, M. Nickel, S. Lund-Katz, G. H. Rothblat, and M. C. Phillips. 2006. Characterization of nascent HDL particles and microparticles formed by ABCA1-mediated efflux of cellular lipids to ApoA-I. *J. Lipid Res.* **47:** 832–843.
43. Liu, L., A. E. Bortnick, M. Nickel, P. Dhanasekaran, P. V. Subbaiah, S. Lund-Katz, G. H. Rothblat, and M. C. Phillips. 2003. Effects of apolipoprotein A-I on ATP-binding cassette transporter A1-mediated efflux of macrophage phospholipid and cholesterol: formation of nascent high density lipoprotein particles. *J. Biol. Chem.* **278:** 42976–42984.
44. Krimbou, L., H. H. Hajj, S. Blain, S. Rashid, M. Denis, M. Marcil, and J. Genest. 2005. Biogenesis and speciation of nascent apoA-I-containing particles in various cell lines. *J. Lipid Res.* **46:** 1668–1677.
45. Maric, J., R. S. Kiss, V. Franklin, and Y. L. Marcel. 2005. Intracellular lipidation of newly synthesized apolipoprotein A-I in primary murine hepatocytes. *J. Biol. Chem.* **280:** 39942–39949.

46. Denis, M., B. Haidar, M. Marcil, M. Bouvier, L. Krimbou, and J. Genest, Jr. 2004. Molecular and cellular physiology of apolipoprotein A-I lipidation by the ATP-binding cassette transporter A1 (ABCA1). *J. Biol. Chem.* **279:** 7384–7394.
47. Gelissen, I. C., M. Harris, K. A. Rye, C. Quinn, A. J. Brown, M. Kockx, S. Cartland, M. Packianathan, L. Kritharides, and W. Jessup. 2006. ABCA1 and ABCG1 synergize to mediate cholesterol export to apoA-I. *Arterioscler. Thromb. Vasc. Biol.* **26:** 534–540.
48. Vaughan, A. M., and J. F. Oram. 2006. ABCA1 and ABCG1 or ABCG4 act sequentially to remove cellular cholesterol and generate cholesterol-rich HDL. *J. Lipid Res.* **47:** 2433–2443.
49. Oram, J. F., G. Wolfbauer, A. M. Vaughan, C. Tang, and J. J. Albers. 2003. Phospholipid transfer protein interacts with and stabilizes ATP-binding cassette transporter A1 and enhances cholesterol efflux from cells. *J. Biol. Chem.* **278:** 52379–52385.
50. Duong, P. T., G. L. Weibel, S. Lund-Katz, G. H. Rothblat, and M. C. Phillips. 2008. Characterization and properties of pre{beta}-HDL particles formed by ABCA1-mediated cellular lipid efflux to apoA-I. *J. Lipid Res.* **49:** 1006–1014.
51. Kee, P., K. A. Rye, J. L. Taylor, P. H. Barrett, and P. J. Barter. 2002. Metabolism of apoA-I as lipid-free protein or as component of discoidal and spherical reconstituted HDLs: studies in wild-type and hepatic lipase transgenic rabbits. *Arterioscler. Thromb. Vasc. Biol.* **22:** 1912–1917.
52. Ishida, B. Y., D. Albee, and B. Paigen. 1990. Interconversion of prebeta-migrating lipoproteins containing apolipoprotein A-I and HDL. *J. Lipid Res.* **31:** 227–236.
53. Miida, T., M. Kawano, C. J. Fielding, and P. E. Fielding. 1992. Regulation of the concentration of pre beta high-density lipoprotein in normal plasma by cell membranes and lecithin-cholesterol acyltransferase activity. *Biochemistry.* **31:** 11112–11117.
54. Kunitake, S. T., C. M. Mendel, and L. K. Hennessy. 1992. Interconversion between apolipoprotein A-I-containing lipoproteins of pre-beta and alpha electrophoretic mobilities. *J. Lipid Res.* **33:** 1807–1816.
55. Babiak, J., H. Tamachi, F. L. Johnson, J. S. Parks, and L. L. Rudel. 1986. Lecithin:cholesterol acyltransferase-induced modifications of liver perfusate discoidal high density lipoproteins from African green monkeys. *J. Lipid Res.* **27:** 1304–1317.
56. Brunham, L. R., J. K. Kruit, J. Iqbal, C. Fievet, J. M. Timmins, T. D. Pape, B. A. Coburn, N. Bissada, B. Staels, A. K. Groen, et al. 2006. Intestinal ABCA1 directly contributes to HDL biogenesis in vivo. *J. Clin. Invest.* **116:** 1052–1062.
57. Dixon, J. L., and H. N. Ginsberg. 1992. Hepatic synthesis of lipoproteins and apolipoproteins. *Semin. Liver Dis.* **12:** 364–372.
58. McCall, M. R., T. M. Forte, and V. G. Shore. 1988. Heterogeneity of nascent high density lipoproteins secreted by the hepatoma-derived cell line, Hep G2. *J. Lipid Res.* **29:** 1127–1137.
59. Chisholm, J. W., E. R. Burleson, G. S. Shelness, and J. S. Parks. 2002. ApoA-I secretion from HepG2 cells: evidence for the secretion of both lipid-poor apoA-I and intracellularly assembled nascent HDL. *J. Lipid Res.* **43:** 36–44.
60. Tsujita, M., C. A. Wu, S. Abe-Dohmae, S. Usui, M. Okazaki, and S. Yokoyama. 2005. On the hepatic mechanism of HDL assembly by the ABCA1/apoA-I pathway. *J. Lipid Res.* **46:** 154–162.
61. Kiss, R. S., D. C. McManus, V. Franklin, W. L. Tan, A. McKenzie, G. Chimini, and Y. L. Marcel. 2003. The lipidation by hepatocytes of human apolipoprotein A-I occurs by both ABCA1-dependent and -independent pathways. *J. Biol. Chem.* **278:** 10119–10127.
62. Denis, M., Y. D. Landry, and X. Zha. 2008. ATP-binding cassette A1-mediated lipidation of apolipoprotein A-I occurs at the plasma membrane and not in the endocytic compartments. *J. Biol. Chem.* **283:** 16178–16186.
63. Faulkner, L. E., S. E. Panagotopulos, J. D. Johnson, L. A. Woollett, D. Y. Hui, S. R. Witting, J. N. Maiorano, and W. S. Davidson. 2008. An analysis of the role of a retroendocytosis pathway in ABCA1-mediated cholesterol efflux from macrophages. *J. Lipid Res.* **49:** 1322–1332.
64. Vedhachalam, C., A. B. Ghering, W. S. Davidson, S. Lund-Katz, G. H. Rothblat, and M. C. Phillips. 2007. ABCA1-induced cell surface binding sites for apoA-I. *Arterioscler. Thromb. Vasc. Biol.* **27:** 1603–1609.
65. Schmitz, G., H. Robenek, U. Lohmann, and G. Assmann. 1985. Interaction of high density lipoproteins with cholesteryl ester-laden macrophages: biochemical and morphological characterization of cell surface receptor binding, endocytosis and resecretion of high density lipoproteins by macrophages. *EMBO J.* **4:** 613–622.
66. Neufeld, E. B., J. A. Stonik, S. J. Demosky, Jr., C. L. Knapper, C. A. Combs, A. Cooney, M. Comly, N. Dwyer, J. Blanchette-Mackie, A. T. Remaley, et al. 2004. The ABCA1 transporter modulates late endocytic trafficking: insights from the correction of the genetic defect in Tangier disease. *J. Biol. Chem.* **279:** 15571–15578.
67. Smith, J. D., C. Waelde, A. Horwitz, and P. Zheng. 2002. Evaluation of the role of phosphatidylserine translocase activity in ABCA1-mediated lipid efflux. *J. Biol. Chem.* **277:** 17797–17803.
68. Takahashi, Y., and J. D. Smith. 1999. Cholesterol efflux to apolipoprotein AI involves endocytosis and resecretion in a calcium-dependent pathway. *Proc. Natl. Acad. Sci. USA.* **96:** 11358–11363.
69. Hassan, H. H., D. Bailey, D. Y. D. Lee, I. Iatan, A. Hafiane, I. Ruel, L. Krimbou, and J. Genest. 2008. Quantitative analysis of ABCA1-dependent compartmentalization and trafficking of apolipoprotein A-I: Implications for determining cellular kinetics of nascent high density lipoprotein biogenesis. *J. Biol. Chem.* **283:** 11164–11175.
70. Lorenzi, I., A. von Eckardstein, C. Cavelier, S. Radosavljevic, and L. Rohrer. 2008. Apolipoprotein A-I but not high-density lipoproteins are internalised by RAW macrophages: roles of ATP-binding cassette transporter A1 and scavenger receptor BI. *J. Mol. Med.* **86:** 171–183.
71. Hamilton, R. L., A. Moorehouse, and R. J. Havel. 1991. Isolation and properties of nascent lipoproteins from highly purified rat hepatocytic Golgi fractions. *J. Lipid Res.* **32:** 529–543.